Cell Reports Sustainability

Article

Identification of pressure points in modern power systems using transfer entropy

Graphical abstract

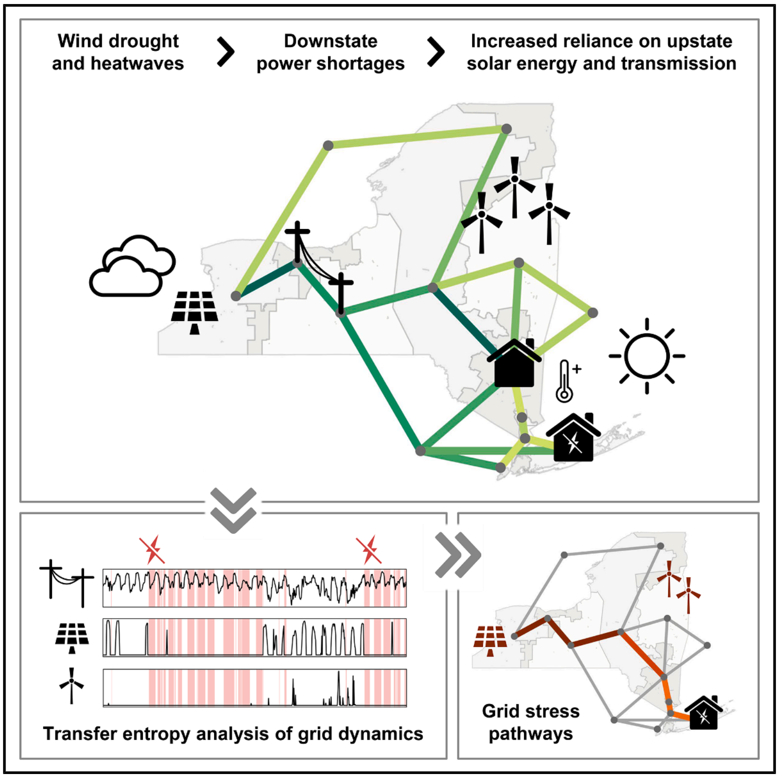

Highlights

- Transfer entropy reveals how grid stress propagates to power shortages
- Reliability failures arise from system-wide interactions, not isolated bottlenecks
- Stress pathways vary across weather and technology scenarios and are hard to predict
- Information-theoretic diagnostics can complement optimization-based planning

Authors

Katerina Tang, M. Vivienne Liu, C. Lindsay Anderson, Vivek Srikrishnan

Correspondence

kbt28@cornell.edu

In brief

Increasing weather dependence in modern power systems introduces reliability risks through complex interactions across generation, transmission, and demand. Tang et al. use transfer entropy to trace how weather-driven system stress propagates to produce power shortages in a proposed future New York State grid. The results reveal non-local, scenario-dependent failure pathways that are difficult to anticipate, highlighting the value of diagnostic, data-driven tools alongside traditional planning models.

Tang et al., 2026, Cell Reports Sustainability *3*, 100660

https://doi.org/10.1016/j.crsus.2026.100660

Cell Reports Sustainability

CellPress
OPEN ACCESS

Article

Identification of pressure points in modern power systems using transfer entropy

Katerina Tang,[1,4,*] M. Vivienne Liu,[2] C. Lindsay Anderson,[1,3] and Vivek Srikrishnan[3]
[1]Center for Applied Mathematics, Cornell University, Ithaca, NY, USA
[2]Systems Engineering, Cornell University, Ithaca, NY, USA
[3]Department of Biological and Environmental Engineering, Cornell University, Ithaca, NY, USA
[4]Lead contact
*Correspondence: kbt28@cornell.edu
https://doi.org/10.1016/j.crsus.2026.100660

SCIENCE FOR SOCIETY Power shortages disrupt daily life, economic activity, and essential services. In modern power systems, weather is an increasingly important driver of reliability: high temperatures raise demand and limit transmission capacity, and calm or cloudy periods reduce wind and solar supply. Using a data-driven analysis, this study identifies grid infrastructure whose operating patterns help predict power shortages. The results show that reliability risks often emerge from interacting stresses across generation, transmission, and demand, rather than from single bottlenecks. By clarifying how system stress propagates through the grid, this diagnostic perspective helps explain why shortages occur under specific conditions and can complement traditional planning and operational tools to support adaptive reliability strategies, targeted monitoring, and coordinated infrastructure investments.

SUMMARY

Integration of variable energy resources—e.g., solar, wind, and hydro—and end-use electrification increase the weather dependence of modern energy systems. Understanding how weather-driven stress propagates through interconnected generation, transmission, and demand is therefore essential for understanding risks and guiding adaptation. We use transfer entropy to identify predictive pressure points: grid components whose utilization dynamics provide predictive information about downstream power shortages. Using simulations of New York State's proposed future power grid across a large ensemble of meteorological and technological scenarios, we show that predictive pressure points frequently emerge from complex, system-wide interactions between generation, transmission, and demand. Importantly, these predictive pressure points vary across scenarios and are often difficult to anticipate from high-level scenario features alone. While transfer entropy cannot establish causality or prescribe optimal infrastructure investments, it offers a complementary, data-driven diagnostic perspective on reliability by revealing how and where system stress propagates under realistic operating dynamics.

INTRODUCTION

The reliability of the electric power system is being impacted by the increasing penetration of variable and intermittent sources of energy generation—such as solar, wind, and hydro—and rising electricity demand due to end-use electrification. Greater penetration of variable generation and electrification increasingly couple the electric power system—across supply, transmission, and demand—with weather, leaving electricity reliability more susceptible to meteorological variability.[1–5]

Given the interconnected nature of the electric power system, shocks from natural stressors across scales (including storms, heatwaves, and longer-scale hydroclimatic trends) can propagate to affect the entire grid.[6–8] Due to the complexity of the power system, it is difficult to predict the dampening or amplification of shocks and where the greatest impacts will be felt.[6,9–11] For example, local decreases in generation due to natural resource variability or deratings due to temperature changes can trigger compensating increases elsewhere, potentially leading to strained supply[3] or transmission line congestion[6] distant from the original disturbance.

The propagation and amplification of shocks due to the complex topology of the electric power grid can lead to the emergence of an operationally critical subset of components[6,10] that we refer to as "pressure points": infrastructure that is consistently associated with the occurrence or severity of power shortages by limiting the system's ability to meet electricity demand. Identifying such pressure points in the power grid can help

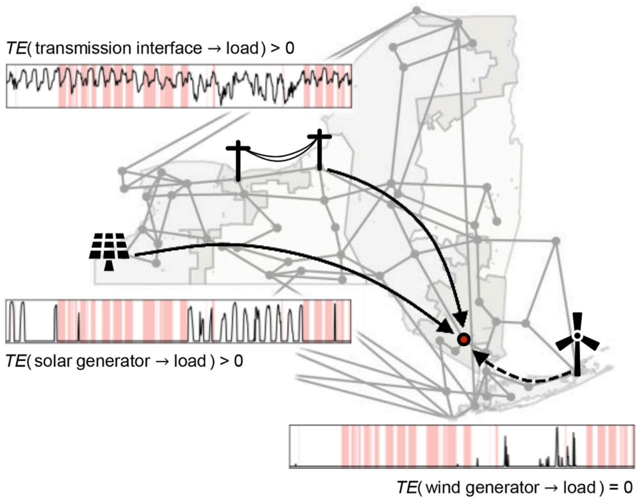

Figure 1. Identifying pressure points in a future NYS grid using TE
We focus on a single load bus (marked in red) and use TE to detect directed, predictive relationships between various components of the grid—wind, solar, and hydro generators; transmission interfaces; and batteries—and this load center. A component is a predictive pressure point if its pattern of utilization improves predictions of future power shortages at the target load bus. Here, interface flow and curtailment are plotted in black for a transmission interface and two generators, respectively, and hours with unmet demand at the target load bus are shaded in red.

characterize patterns of system vulnerability and reveal how stress propagates across interconnected generation, transmission, and demand. However, because these pressure points may be geographically or topologically distant from both the original shock(s) and where electricity demand is unmet,[6,9] they can be hard to identify from patterns of local shortages or transmission line congestion.

Furthermore, natural meteorological variability does not necessarily cause abrupt component outages but can stress or weaken the power grid over extended periods by simultaneously reducing weather-dependent energy generation output, limiting transmission, and increasing electricity demand.[3,5] This is in contrast with acute failures of grid components, which is a common setting for previous work on identifying critical infrastructure in power grids. Some approaches adapt classical network centrality measures to power-system settings and assess component importance based on the system-level impacts of node or line outages.[12–16] Other works analyze the statistical relationships between the topological properties of nodes or links and the dynamics of simulated cascading failures triggered by their removal.[10,17] However, when individual components—or multiple, spatially correlated components—remain operational but at reduced capacity, the impacts on the power grid are more difficult to trace or quantify, especially as other components can compensate to help meet demand and largely avoid power outages.[6] We focus on identifying pressure points in this setting, where reliability risks arise from compound interactions among generation, transmission, and demand rather than from discrete component failures.

One class of approaches to identifying pressure points infers component criticality indirectly using prescriptive modeling frameworks, such as capacity expansion or transmission expansion models, which prioritize investments that most efficiently improve system reliability.[18–21] In many capacity expansion formulations, reliability is incorporated either by pricing unserved load,[22,23] leading to an explicit cost-reliability trade-off in the objective function, or by imposing adequacy constraints that require minimum reliability standards be met.[19,20,24] Generation, transmission, and/or storage capacities are treated as decision variables subject to operational and policy constraints, and cost and reliability metrics are evaluated under counterfactual system designs. Within these optimization-based frameworks, the associated dual variables for capacity or flow constraints measure the value of expanding the corresponding components, providing a principled basis for prioritizing investments in power system planning studies.

While such optimization-based approaches are indispensable for infrastructure planning, they may not reveal the pathways by which stressors result in outages or the conditions under which particular reliability challenges emerge. Less attention has so far been paid to diagnostic, data-driven methods that characterize how stress propagates through a fixed system realization under realistic operational dynamics and that identify which components provide early signals of downstream reliability failures. Such an approach would help us understand how limitations upstream in the power system propagate downstream to outages, and this is particularly important in power systems with high penetrations of variable and intermittent energy sources, where reliability challenges can emerge from compound, system-wide interactions rather than from the failure or full utilization of a single infrastructure component.

In this study, we adopt the latter perspective: we identify potential pressure points by inferring directed predictive relationships between the utilization dynamics at supply- and transmission-side infrastructure (including generators, transmission interfaces, and batteries) and unmet demand at a specific load bus. These inferences are based on hourly time series data reflecting resource utilization and unmet demand in simulated power flow studies.

Such directed dependencies define a form of effective network connectivity[25,26] in which components are linked not by physical electrical connections but by their influence on future system behavior. Accordingly, we define a "predictive pressure point" as any generation, transmission, or storage component whose utilization dynamics provide statistically significant predictive information—quantified in this study using transfer entropy (TE)[27]—about future unmet demand at a given load bus (Figure 1). Framing the problem in this way aligns with a broader literature using data-driven techniques to discover underlying grid interactions that may not be evident from direct or proximal electrical connections.[9,11,28,29]

TE, our metric of effective network connectivity, is an information-theoretic measure that can detect directed, potentially nonlinear predictive relationships between components in a system[25] (see methods for details). TE quantifies the extent to which knowledge of the past state(s) of one process, X, improves predictions of the future state of another process, Y, *beyond* what is already predictable from Y's own past. A positive TE from X to Y therefore suggests that the dynamics of X provide unique predictive information about the future evolution of *Y*, and although this does not establish causality, it reflects a meaningful directional dependence. TE is zero when the two processes are completely independent or when *Y*'s own past already contains all the relevant information in *X*, i.e., the two processes are perfectly coupled (Figure S1). As evidence of its wide applicability, TE has been used to infer effective network connections from time series data in neuroscience,[26,30] climatology,[31] urban land teleconnections,[32] and econometrics.[33] To the best of our knowledge, this is the first study to apply TE as a diagnostic tool for identifying failure pathways in power systems.

We demonstrate our approach using a proposed future New York State (NYS) power grid, as described and scoped by the state's Climate Leadership and Community Protection Act (CLCPA).[34] The CLCPA is an ambitious energy agenda that targets 70% non-fossil electricity by 2030, 100% zero-emission electricity by 2040, and eliminating emissions statewide by 2050. To meet these emission targets, the scoping plan calls for integrating additional variable and intermittent energy sources (e.g., on- and offshore wind and utility and behind-the-meter solar), upgrading and expanding transmission infrastructure, and electrifying end uses such as transportation and heating/cooling.[34] However, this plan exacerbates the spatial imbalance between energy supply, which is concentrated in upstate NYS (Figure S2), and load, which is concentrated downstate, primarily in New York City. Because of this imbalance—especially the uneven distribution of energy resources—NYS experiences complex responses to meteorological variability, making the future NYS grid a valuable case study for understanding the reliability risks of grids with intermittent resources.[2,35]

This study employs simulations from ACORN (A Climate-informed Operational Reliability Network),[2] a simplified optimal power flow (OPF) model of the proposed 2040 NYS grid, and connections to neighboring grids. These simulations were generated under scenario assumptions reflecting different meteorological forcings—primarily temperature increases—and levels of variable energy penetration and electrification. Hourly energy generation, transmission interface flow, battery state, and unmet demand are calculated for each meteorological-technological scenario by determining the optimal dispatch of resources to minimize power shortages (see methods for details of the model, scenario design, and data-generating process).

In the first part of this study, we examine predictive pressure points in three specific scenarios representing distinct meteorological and technological challenges to the future NYS grid. Previous studies of the reliability dynamics in future NYS grids[2,35] help us reason about the broad categories of pressure points that we might expect to see in each scenario. These insights allow us to confirm that the specific predictive pressure points identified by TE largely align with known reliability challenges[2,35] and are consistent with expected system behavior. Importantly, predictive pressure points can also reveal complex and sometimes unexpected interactions between generation and transmission patterns that ultimately lead to unmet demand. This highlights how interconnected the generation and transmission systems are in a grid with intermittent energy resources, underscoring the importance of analyzing these components jointly when assessing reliability risks.

We then extend our analysis to all 6,600 meteorological-technological scenarios in the full ensemble, identifying predictive transmission pressure points in each and clustering the results to uncover shared system dynamics. From a decision-making perspective, a key question is whether these pressure points can be anticipated from high-level indicators of grid conditions—e.g., temperature, resource availability, or installed capacity—so that planners can proactively design for reliability. However, we find that these broad scenario features offer limited predictive power, reinforcing the conclusion of the preceding analysis: predictive transmission pressure points arise from complex, system-wide interactions among generation, transmission, and demand across spatial and temporal scales. This unpredictability highlights the potential value of adaptive approaches and real-time system monitoring for understanding and managing reliability risks in future power systems.

RESULTS

Heterogeneous grid dynamics across meteorological-technological scenarios

One persistent challenge in using TE to identify networked impacts is that TE is a measure of network correlation, not causation.[25,30] This means that predictive pressure points could hypothetically be the result of spurious correlations rather than meaningful causal patterns. To evaluate the plausibility of these inferences, we analyze three scenarios spanning a range of meteorological and technological assumptions (see Figure 2) in more depth. In each case, we evaluate the identified predictive pressure points in the context of previous studies,[2,35] known structural features of the NYS grid, and the relatively simple power flow dynamics observed in ACORN.

A key structural feature of the CLCPA's proposed NYS grid is the spatial imbalance between energy supply and electricity demand, which ACORN simulations consistently demonstrate is a major challenge for grid reliability.[2,35] To meet the zero-emissions generation target by 2040, the CLCPA scoping plan[34] prescribes wind, solar, and hydro resource capacities across the eleven New York Independent System Operator (NYISO) load zones (A-K; Figure S2), totaling 26.4 GW of wind (land-based and offshore), 51.2 GW of utility solar, and 4.3 GW of hydropower. Most planned land-based wind, utility solar, and hydropower resources are located upstate—in zones A through E—and in zone F. Meanwhile, electricity demand is disproportionately concentrated downstate in zones J and K, which have primarily offshore wind generation resources. As a result, power typically flows from upstate to downstate, and the upstate-to-downstate transmission corridor—particularly the E-G interface—is a persistent bottleneck, including in the three meteorological-technological scenarios we consider here (Figure 2C).

We first examine a relatively "well-behaved" scenario in which energy availability is high—largely because total installed wind and solar capacities are 126% and 135%, respectively, of CLCPA targets—and the assumed temperature increase is moderate (Figures 2A and 2B). These favorable conditions reduce overall strain on the system, yet we see some pressure points still emerge, and in particular, downstate power shortages occur exclusively during hours in which the critical E-G interface is

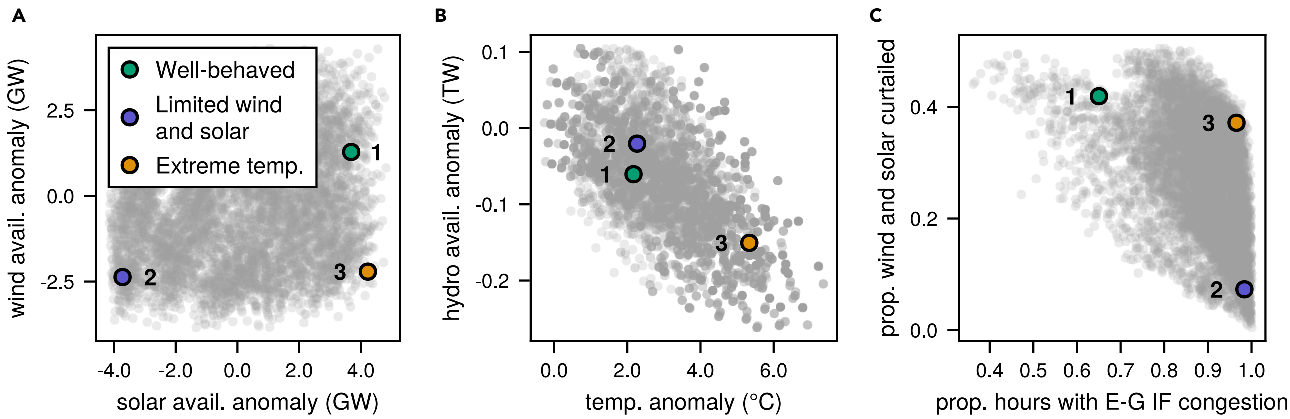

Figure 2. Meteorological and technological features of three chosen scenarios in the context of the full scenario ensemble

Colored markers indicate the three selected scenarios within the full ensemble (gray points), illustrating distinct combinations of meteorological and technological conditions. More information about the three selected scenarios is available in Table S1.

(A) Time-averaged wind and solar availability anomalies, expressed as mean hourly deviations from a baseline scenario (see methods for definitions of anomalies and baseline scenario).

(B) Time-averaged temperature and hydropower availability anomalies, where temperature anomalies are mean hourly deviations and hydropower anomalies are mean quarter-monthly deviations from the baseline.

(C) Reliability-relevant outcomes in each scenario, summarized by the proportion of wind and solar generation curtailed and the proportion of hours with congestion on the E-G interface, a key bottleneck in the upstate-to-downstate transmission corridor.

congested. However, this congestion does not appear to be a major barrier to the effective use of available energy resources: wind and solar curtailment upstate, congestion of the E-G interface, and unmet demand downstate co-occur in less than 9% of simulated hours. Instead, the large volume of curtailed wind and solar generation (20.4 TWh) compared with a much smaller total power shortage (1.29 TWh) points to a temporal mismatch between when these intermittent energy resources are available and when they are needed.

Next, we consider two more extreme meteorological-technological scenarios in which statewide energy availability is more constrained. In the first of these two scenarios, wind and solar capacities are only 73% and 63%, respectively, of what is called for in the CLCPA scoping plan, but the temperature increase is still fairly moderate (Figures 2A and 2B), and we refer to this scenario as the "limited wind and solar" scenario. The third and final scenario has relatively limited wind availability and a large temperature increase (Figures 2A and 2B). This extreme temperature increase depresses hydropower availability (Figure 2B) and reduces transmission ampacity[36] while dramatically increasing overall demand due to increased cooling load (Figure S3). Total statewide load over the entire simulation period is 121% of the baseline (see methods for details of the baseline scenario), with hourly load peaking at 147% of the baseline.

The extreme conditions in the second and third scenarios—particularly the limited offshore wind availability—result in a greater reliance on upstate energy supply to meet downstate demand, exacerbating congestion in the upstate-to-downstate transmission pipeline. As a result of transmission constraints, a large proportion of available upstate wind and solar generation—most notably in the third scenario—cannot be delivered to load centers downstate and is therefore curtailed, even as unmet demand persists. This congestion-driven underutilization of already scarce energy resources contributes to power shortages[2] and higher system costs.[35] It also intensifies generation-side pressure points as constrained supply struggles to keep pace with electricity demand, particularly under extreme temperature conditions.

Pressure points emerge from interactions between generation and transmission

Throughout our TE analysis, we focus on identifying pressure points that help predict power shortages at a bus located in zone G (highlighted in Figure 3). This bus lies along the critical (and frequently congested) upstate-to-downstate transmission pipeline and consistently exhibits the highest frequency and largest share of unmet demand across the entire scenario ensemble (Figure S4). While electricity demand peaks further downstate, particularly in New York City and Long Island (zones J and K, respectively), shortages in those zones tend to co-occur with shortages at the zone G bus: in over 99% of scenarios, at least 90% of hours with unmet demand in zones J and K coincide with hours of unmet demand at this zone G location. This makes it a strategically informative site for identifying system-wide predictive pressure points.

In the well-behaved scenario (Figure 3A), our TE analysis highlights temporal mismatches between intermittent energy generation and load as the primary drivers of power shortages. Most predictive pressure points are generators where available wind and solar resources are consistently fully utilized—i.e., no curtailment occurs—during periods of unmet demand at the target load bus (Figure S5A). Shortages are heavily concentrated during hours in which wind and solar availability at these sites drops below 50% of nameplate generation capacity (Figure 4A), particularly at night when solar is unavailable and when wind availability is also reduced. Together, these observations reinforce the

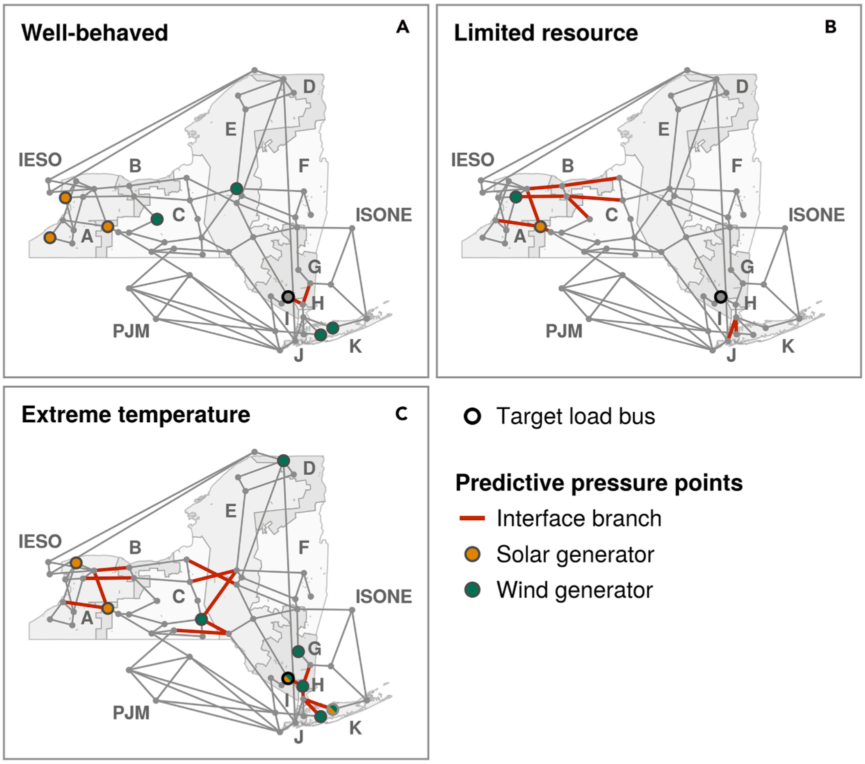

Figure 3. Predictive pressure points identified by pairwise TE analysis

Predictive generation and transmission pressure points identified in the (A) well-behaved scenario, (B) limited wind and solar scenario, and (C) extreme temperature scenario. The target load bus in all three scenarios is in zone G, circled in black. For predictive transmission pressure points, all branches comprising the interface are colored red.

interpretation that timing, rather than supply capacity, is the key driver of supply-side pressure points in this scenario.

The G-H interface is also flagged as a predictive pressure point (Figure 3A) due to diurnal decreases in interface flow that are predictive of power shortages at the target load bus in zone G (Figure S6A). However, this predictive relationship is likely spurious: an underlying driver of both unmet demand in zone G and G-H interface flow dynamics appears to be low solar availability in zone F (Figure S6B), which has the state's largest share of utility solar resources and contributes heavily to downstate energy supply. Because the E-G interface is frequently congested (Figure 2C), solar generation in zone F and flow across the F-G and G-H interfaces become critical for meeting demand in zones G through K, amplifying the predictive role of the G-H interface. We return to this issue of common drivers and the interpretability of bivariate TE in the discussion.

Overall, these dynamics are consistent with system conditions in which expanded energy storage could play a role in addressing the temporal mismatches between energy supply and electricity demand that occur in grids with high penetrations of non-dispatchable, intermittent energy resources.[37] In over half of simulated hours, curtailment of wind and solar generation co-occurs with fully met demand. Long-duration batteries as well as more flexible, even-longer-duration options such as green hydrogen could make more efficient use of the abundant but intermittent energy resources in this scenario.[2]

Notably, the E-G interface is not identified as a predictive pressure point in this scenario despite being a known structural bottleneck.[2,35] This is a consequence of its near-deterministic relationship with downstate power shortages in this scenario: unmet demand downstate is so strongly correlated with congestion of the E-G interface that the interface flow contains little unique predictive information. We consider this specific limitation of TE as a metric of effective network connectivity in the discussion.

In the second scenario we examine—the limited wind and solar scenario—our TE analysis also identifies supply-side predictive pressure points (Figure 3B). However, here the predictive relationship reflects a more fundamental supply constraint: at flagged generators, wind and solar resources are again fully utilized during hours of unmet demand (Figure S5B), but unlike the well-behaved scenario, power shortages are not limited to periods of extremely low energy availability (Figure 4B). This aligns with our expectations for this meteorological-technological scenario, in which underbuilt wind and solar generation capacity leaves the grid susceptible to ordinary meteorological variability such that even moderate decreases in wind or solar availability can lead to shortages.

Another consequence of underbuilt offshore wind in particular is the increased reliance on far-upstate energy resources, particularly the considerable hydropower and utility solar resources located in zone A. As discussed previously, this exacerbates congestion along the upstate-to-downstate transmission corridor, and we see that the A-B and B-C interfaces are identified as predictive pressure points (Figure 3B). These interfaces see extended periods of high utilization and congestion during shortage hours, averaging 90% and 97% of transmission capacity, respectively, compared with 77% and 90% during periods with no power shortage at the target bus (see also Figures S7A and S7B). Notably, these interfaces are geographically and electrically distant from the target bus, underscoring TE's ability to surface these system-level interactions between generation and transmission rather than only proximate or isolated drivers.

Taken together, these findings indicate that reliability failures in this scenario arise from interacting generation and transmission constraints rather than from a single dominant bottleneck. When demand goes unmet in zone G, upstream resources are typically fully utilized: curtailment of wind and solar generation in zones A and B is rare, occurring in only 13% of all simulated hours and 4% of shortage hours. At the same time, congestion

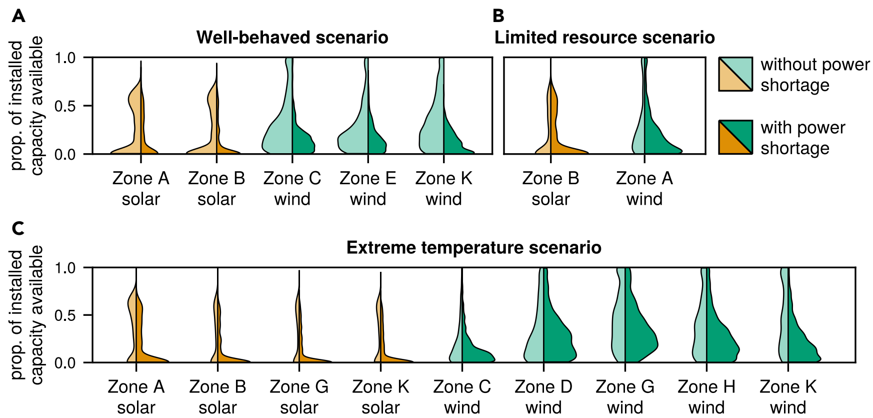

Figure 4. Distribution of generation availability relative to installed capacity at identified predictive pressure points

In each panel, hours with zone G power shortages and without zone G power shortages are plotted on the right and left, respectively. All predictive generation pressure points identified within a single zone have been aggregated.
(A) Well-behaved scenario.
(B) Limited wind and solar scenario.
(C) Extreme temperature scenario.

of the B-C interface, which is fully utilized in 70% of shortage hours, limits the deliverability of upstream resources. The joint scarcity of flexible supply and transmission capacity defines this failure pathway linking far-upstate resources to downstate power shortages.

The I-J interface is also identified as a predictive pressure point in this limited wind and solar scenario, reflecting a more subtle but still physically interpretable connection. Here, a consistent pattern of peaking interface flow from zone I to zone J—which has the largest electrical load among all NYISO zones—is predictive of unmet demand at the target load bus in zone G (Figure S7C). These peaks in interface flow largely occur during hours with low offshore wind availability in zone J (Figure S8A). When offshore wind availability is high, shortages in zone J can largely be avoided—98% of hours with unmet demand in zone J coincide with wind availability below 50% of zone J's installed capacity—and the reverse flow of power from zone J to zone I can help meet demand elsewhere, including in zone K and indirectly in zone G (Figure S8B). While power does not ever flow in the I → H direction, i.e., from downstate to upstate, this pattern underscores the broader system-wide importance of downstate energy supply and transmission flexibility in shaping reliability outcomes. Notably, this is a relationship that a simple correlation analysis would likely miss, and TE captures the predictive value of more complicated flow patterns—such as peaks—rather than steady levels or direction alone.

In the final scenario, extreme temperatures significantly increase electricity demand while decreasing hydropower availability, and wind availability is also decreased (Figures 2A and 2B). The grid becomes heavily reliant on solar generation—particularly from upstate zones and zone F—to meet this elevated load. As a result, the predictive transmission pressure points observed in the previous scenarios become more prominent (Figure 3C). For example, A-B interface congestion once again emerges as a strong predictor of downstate power shortages (Figure S9A), occurring in 36% of hours with unmet demand in zone G but only 7% of hours with no unmet demand. Diurnal fluctuations in interface flow are more pronounced here than in the two previously discussed scenarios, reflecting the system's increased dependence on zone A's solar generation in the absence of dispatchable hydropower.

More predictive transmission pressure points emerge along the upstate-to-downstate transmission pipeline—specifically at the C-E, G-H, and H-I interfaces (Figures S9B–S9D). As in the well-behaved scenario, these pressure points reflect a common driver: diurnal solar variability. Lower interface utilization during periods of solar unavailability corresponds to unmet demand in zone G. When solar supply—particularly in zones C and F—are sufficient, these interfaces are more fully utilized and shortages are reduced. This pattern illustrates that congested transmission can be primarily a consequence of power flow dynamics and does not necessarily indicate a bottleneck or limitation in the system but rather that available resources are being utilized appropriately to meet load.

Supply-side predictive pressure points are also widespread in this scenario (Figure 3C), reflecting the broader challenge of meeting elevated demand under extreme temperature increases. Many of these predictive pressure points occur at wind generators, and notably, power shortages occur even when wind availability reaches installed capacity (Figure 4C), indicating that available wind resources are frequently fully utilized during shortage events. This pattern suggests that wind capacity across the state may be underbuilt relative to the total load. However, because much of the existing land-based wind relies on long-distance transmission through already stressed upstate interfaces, additional land-based capacity would likely be less effective at mitigating shortages than offshore wind located closer to downstate load centers.

The importance of these spatial considerations is further underscored by curtailment patterns. At a solar generator in zone A flagged as a predictive pressure point, generation is curtailed in about 8% of hours with unmet demand in zone G (bottom panel of Figure S5C). More broadly, curtailment occurs somewhere in the system in about 64% of hours with unmet demand, indicating that transmission constraints frequently limit the effective use of available upstate energy resources to meet downstate demand. These findings highlight the importance of considering generation expansion and transmission upgrades in tandem.

The final predictive pressure point in this scenario is the I-K interface. Here, periods of sustained flow in the K → I direction predict power shortages in zone G (Figure S10A). This pattern reflects increased reliance on offshore wind from zone K to support demand in zone J, particularly when overall energy supply from upstate is reduced (Figures S10B and S10C). However, unlike

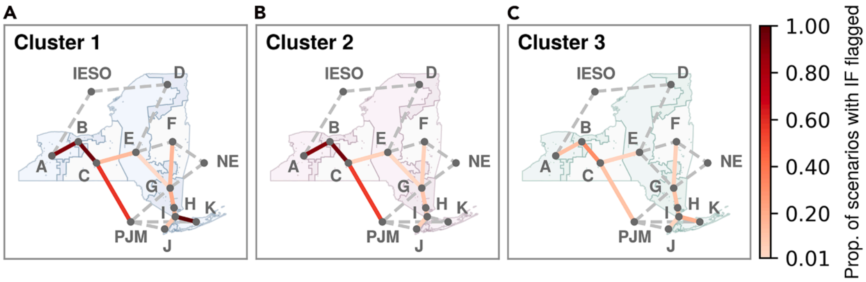

Figure 5. Patterns of predictive transmission pressure points grouped into three clusters

Common predictive transmission pressure points in (A) cluster 1, (B) cluster 2, and (C) cluster 3. Interfaces are colored according to the proportion of scenarios belonging to that cluster in which the interface is flagged as a predictive transmission pressure point, and interfaces flagged in less than 1% of scenarios are drawn in dashed gray lines. Note that the NY-PJM interface connects zone C and the PJM ISO but does not include connections from the PJM ISO to zones G, J, and K.

the dynamics of the I-J interface observed in the previous scenario—where reverse flow helped mitigate zone G power shortages—here K → I flow is insufficient to prevent zone G shortages. This is likely due to the relatively low interface flow limit in the K → I direction (515 MW), which is much smaller than zone J's mean hourly load (approximately 8,950 MWh). Still, the dynamics of this pressure point are consistent with the broader system condition: underbuilt wind, strained solar supply, and overwhelming downstate demand.

Transmission pressure points are hard to predict based on meteorological and technological features

In the previous subsection, we demonstrated that predictive pressure points reflect diverse and often complex system dynamics that can vary across meteorological and technological conditions. This raises two decision-relevant questions. First, which predictive pressure points—if any—are common across a broad range of meteorological-technological scenarios? Second, can the emergence of specific pressure points be anticipated from broader operating conditions, allowing planners to anticipate and monitor for reliability risks in advance? This process—identifying the underlying scenario features that result in similar system dynamics—is known as scenario discovery[38] and can help guide decision-makers in planning for system reliability under uncertainty.

To investigate the first question, we group the 6,600 meteorological-technological scenarios based on similarities in their transmission-level predictive pressure points, which, as demonstrated above, capture critical reliability dynamics often overlapping with those suggested by generation-level predictive pressure points. A clustering analysis (see methods for details) reveals three distinct clusters of scenarios, each characterized by a common spatial pattern of predictive transmission pressure points (Figure 5). That is, each cluster contains scenarios where similar subsets of transmission interfaces emerge as predictive pressure points, pointing to similar modes of system failure. Scenarios in the first two clusters share multiple predictive pressure points, namely, the A-B and B-C interfaces, while the third cluster contains more variable, scenario-specific patterns.

In the first and second clusters, unmet demand in zone G is frequently associated with periods of high utilization and congestion at the A-B and B-C interfaces (Figures S11A and S11B). This pattern suggests that predictive pressure points emerge along the entire upstate-to-downstate transmission corridor—crucially, also upstream of the well-known bottleneck at the E-G interface. Although the E–G interface is frequently or almost always congested across all scenarios (Figure 2C) and has been previously identified as a critical bottleneck,[2,35] its persistent congestion typically renders it non-predictive in this analysis (see discussion).

The interface connecting NYS to the neighboring PJM system also emerges as a common predictive pressure point in these clusters. In these scenarios, flow from NYS to PJM exhibits a strong diurnal pattern (Figure S11C) reflecting daily fluctuations in downstate demand. This pattern reflects the NYS-PJM interface's important role in moving net power from upstate to downstate—critically, bypassing the bottleneck at the E-G interface—during periods of system stress.

The first and second clusters are primarily distinguished by the presence of the I-K interface as a predictive pressure point in the first cluster but not in the second. Among the scenarios in which the I-K interface is identified as a predictive pressure point, we observe two distinct dynamics connecting I-K interface flow and power shortages in zone G. In some scenarios, power shortages in zone G align with elevated interface flow in the I → K direction, while elevated interface flow in the K → I direction helps mitigate power shortages (Figure S12A). In other words, power moving out of zone K during hours with excess offshore wind generation helps the system meet demand in zone G, likely indirectly by balancing demand in zone J.

Other scenarios show persistent congestion and high interface flow in the K → I direction, regardless of shortages in zone G (Figure S12B). These scenarios are also characterized by increased flow from zone H to zone I, indicating overall higher downstate demand that draws heavily on external resources from other zones, both upstate zones and zone K (Figure S12C). Under such conditions, exporting surplus electricity from zone K does not sufficiently reduce demand to prevent shortages in zone G, and this is what we saw in the third, extreme temperature scenario examined previously.

To better understand what drives the emergence of these distinct predictive pressure point patterns, we examine whether cluster membership can be predicted from high-level meteorological and technological features of each scenario. That is, we use a classification tree[39] to examine to what extent broad weather and infrastructure conditions can account for the different types of reliability dynamics observed. We consider five key variables in each scenario: the mean anomaly relative to a baseline scenario with historical meteorological patterns

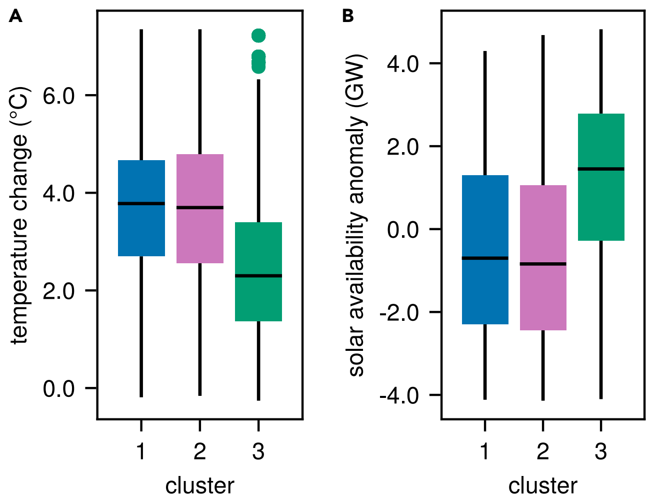

Figure 6. Temperature change and relative solar availability for three identified clusters

The cluster numbers correspond to those in Figure 5. Boxplots summarize the distribution of mean hourly deviations in (A) average statewide temperature and (B) statewide solar availability relative to a baseline scenario (see methods for details of the baseline scenario).

for four different metrics—hourly temperature averaged across the state, hourly solar availability, hourly wind availability, and quarter-monthly hydro availability—as well as the battery capacity scaling factor. In principle, these features reflect major drivers of electricity supply and demand and should help explain observed differences in predictive transmission pressure points. However, a basic classification tree[39] trained to predict cluster membership achieves only 51.4% accuracy—only slightly better than random guessing (see methods for details).

Still, examining the most influential predictors in the classification tree—the mean hourly anomaly in temperature and solar availability—reveals some broad connections between specific meteorological-technological features and reliability dynamics. Scenarios comprising the first and second clusters tend to have larger temperature increases—and therefore higher levels of electricity demand and lower availability of hydropower—combined with lower solar availability (Figure 6). With simultaneously higher load concentrated downstate and relatively low solar availability, the grid is likely more reliant on upstate land-based wind and hydropower. This leads to pressure points at key upstate-to-downstate transmission interfaces—both moving power out of zones A and B and moving power through PJM in order to bypass the frequently congested E-G interface. However, the first and second clusters remain largely indistinguishable, even when considering the full set of features.

Scenarios belonging to the third cluster tend to have higher solar availability relative to the level of temperature increase. As a result, these scenarios can be considered more well-behaved, and the sets of predictive pressure points that emerge are less systematic and more scenario-specific.

Overall, the limited predictive power of these features emphasizes that predictive transmission pressure points arise from complex interactions between generation, transmission, and demand across space and time. More granular metrics that better capture the spatiotemporal patterns of intermittent energy resources and electricity demand may offer better predictive insight. In the meantime, these results highlight the value of real-time grid monitoring and underscore the need for flexibility in reliability planning. Efforts to enhance grid reliability should remain adaptive, with strategies that can respond to evolving meteorological and technological conditions.

DISCUSSION

Across a wide range of technological and meteorological conditions, our TE analysis consistently identifies common predictive pressure points that reflect potentially persistent failure modes in a future NYS grid. In particular, predictive pressure points for downstate power shortages frequently emerge at transmission interfaces and generation sites along the entire upstate-to-downstate transmission corridor. Many of these predictive pressure points are geographically and electrically distant from where the power shortages actually occur, and this reinforces previous observations that the complexity of the electric power system can result in a spatial separation between the affected generation or transmission infrastructure and where demand is unmet.[6]

Predictive pressure points emerge from interactions between generation and transmission under system stress, particularly during periods of elevated demand—largely driven by higher temperatures—and limited energy availability. Analyzing power flow dynamics at these transmission pressure points can be quite complex: for example, many power shortage events occur when transmission lines are not congested, which may seem counterintuitive. In such cases, reduced utilization reflects insufficient upstream generation, leaving the transmission paths underutilized, rather than excess transmission capacity. This adds nuance to the common use of line congestion as a signal of reliability failures.[2,6,35] By capturing directed, time-lagged dependencies between component utilization and unmet demand, TE helps reveal how reliability failures emerge through the temporal sequencing and spatial propagation of stress across the network—dynamics that are difficult to infer from static component-level indicators alone.

We note that TE is fundamentally a diagnostic tool: while it identifies components whose utilization patterns carry predictive information about impending power shortages, it cannot quantify the marginal reliability benefit of potential interventions or allow a prescriptive ranking of investment priorities. This distinction is illustrated by the frequently congested E-G interface, a well-documented bottleneck in the NYS grid[2,35] that is rarely identified as a predictive pressure point in our analysis. Despite its physical connection to our target load bus and its established role as a binding constraint, the E-G interface is flagged as a predictive pressure point in less than 2% of the full scenario ensemble. In many scenarios, persistent congestion of the E-G interface produces minimal temporal variability in interface flow, limiting its predictive value. In other scenarios, power shortages at the load bus are primarily the direct result of congestion in the E-G interface, and the occurrence of power shortages is almost perfectly correlated with congestion such that the history of unmet demand already encodes nearly all the information contained in the interface flow history (see Figure S13). In both cases—near-constant behavior or near-deterministic coupling—the incremental predictive information measured by TE is necessarily small.

Importantly, this example should not be interpreted as a sign that the E-G interface is not structurally critical. Rather, this example highlights that predictive pressure points and structurally limiting constraints need not coincide. Understood this way, TE analysis complements prescriptive planning frameworks (e.g., capacity expansion models) by offering a data-driven, diagnostic perspective on reliability that reveals how and where system stress propagates within a fixed system configuration. For example, in the well-behaved scenario, shortages are primarily associated with temporal mismatches between intermittent generation and demand rather than absolute shortages of installed capacity—an operational pattern consistent with planning studies that emphasize the value of storage[37] and dispatchable backup generation capacity.[21] In the more extreme scenarios, predictive pressure points reflect intertwined generation and transmission constraints, highlighting reliability challenges that arise from coupled system dynamics rather than from a single limiting component. Longer-range flexibility options such as green hydrogen, which can shift energy without relying on congested transmission, may be relevant in such settings.[2]

TE's diagnostic perspective may be particularly valuable when paired with planning frameworks designed to generate diversity in candidate system designs rather than to identify a single optimal solution. For example, modeling to generate alternatives[40,41] (MGA) is explicitly intended to explore the feasible, near-optimal region of the solution space, producing system designs that remain high-performing with respect to modeled objectives (e.g., cost and reliability) while being maximally different in their specific infrastructure configurations. In this spirit, TE could serve as a complementary diagnostic layer applied after MGA alternatives are generated to highlight system configurations where reliability is statistically informed by non-local interactions or by specific upstream components.

It is worth emphasizing some limitations of our approach. First, demand response is not explicitly considered in this analysis. We choose to prioritize being able to meet all demand, so we do not examine electrical loads at other buses as potential predictive pressure points. Future work will study the role of demand-side stresses and interventions.

Beyond modeling choices, there are also practical considerations related to the estimation and application of TE itself. Reliable estimation of TE requires sufficiently long, high-resolution time series to adequately sample the underlying joint probability distributions of embedded source and target processes.[25] For continuous-valued signals, state-of-the-art estimators typically rely on repeated high-dimensional nearest-neighbor searches, which increase in computational cost with data length and embedding dimension.[26,42] In addition, statistical validation via surrogate-based testing must be performed independently for each candidate interaction[30] (see methods for details of TE estimation). Together, these requirements imply meaningful data and computational demands, particularly for large systems or very high-dimensional analyses. However, they are tractable in settings where long, well-resolved operational time series are available—such as the simulation-based power system analyses considered here—and where TE is used as a targeted diagnostic rather than as an exhaustive network reconstruction tool.

Recovering the full set of interactions among infrastructure components would require estimating multivariate transfer entropies,[43,44] which account for redundant influence and detect synergistic (higher-order) interactions by conditioning on more than one source process simultaneously.[25] Our pairwise analysis therefore necessarily risks both false positives due to common drivers and false negatives where predictive information arises only jointly from multiple components. An example of a redundancy-driven false positive appears in the well-behaved scenario: solar availability upstream, particularly in zone F, drives both power shortages in zone G and the dynamics of flow through the G-H interface, creating a false predictive relationship from G-H interface flow to power shortages in zone G. Conversely, we almost surely overlook some synergistic interactions—most notably, the role of batteries in helping compensate for transmission congestion and intermittent energy resources. Across the three narrative scenarios, batteries are never identified as predictive pressure points, likely because their own dynamics are closely tied to transmission constraints: discharging batteries upstream of interface congestion cannot help relieve power shortages in zone G, and depleted batteries downstream of transmission congestion cannot be recharged. Estimating a multivariate TE that conditions jointly on battery utilization and intermediary interface congestion could potentially reveal this synergistic interaction between storage and interface flow as a predictive pressure point in the system.

In principle, a multivariate TE analysis could address the fundamental limitations of our pairwise analysis, but a brute force approach would likely be computationally intractable given the combinatorial explosion in the number of potential sets of candidate sources.[43] Existing methods for full network inference via multivariate TE[43–45] therefore construct the conditioning set of relevant source processes iteratively, typically using a greedy approach. These methods are substantially more computationally intensive than a pairwise analysis, requiring many TE estimates and tests for statistical significance, and may therefore be impractical for large power systems. In future work, it is worth considering how domain knowledge—e.g., physical constraints and grid topology—may be helpful in thoughtfully expanding the set of relevant source processes, thereby reducing computational burden while preserving interpretability. It is also worth exploring whether alternative methods of reconstructing networks from time series data[46–48] may offer more scalable or robust diagnostics in this context.

Despite these limitations, this analysis has demonstrated that TE can be a valuable diagnostic tool for identifying predictive infrastructure pressure points that emerge from complex, system-wide interactions between generation and transmission patterns in a grid weakened by natural stressors. By focusing on directed, time-lagged relationships in operational dynamics, our approach reveals non-local and scenario-dependent failure pathways that are difficult to detect using static metrics or outage-based analyses. Across a large ensemble of meteorological-technological scenarios, we show that these predictive pressure points are heterogeneous and often cannot be anticipated from coarse summaries of grid operating conditions, highlighting the limits of relying on aggregated indicators to assess reliability risk. Framed appropriately, TE (or other information-theoretic network analyses) complements prescriptive planning and optimization frameworks by helping to interpret where and how stress propagates through a fixed system realization, thereby providing context for understanding why particular classes of interventions may be emphasized under different operating conditions.

METHODS

Model and scenario design

We use a scenario ensemble generated by ACORN,[2] a reduced-form direct current OPF (DC-OPF) model of the proposed 2040 NYS power grid outlined in the CLCPA scoping plan.[34] The scoped plan includes (relative to the present-day NYS grid[49]) expanded variable energy generation and transmission capacity, new high-voltage direct current lines, and additional load due to electrification of transportation and heating/cooling sectors.

As grid reliability is heavily influenced by the joint behavior of temperature (which affects demand and transmission ampacity) and energy supply (solar, wind, and hydro), it is important for operational assessments to use realistic joint distributions of these meteorological inputs. To maintain their co-variability, we force the simulations using reanalysis weather data from MERRA2 over the 22-year simulation period (1998–2019). The DC-OPF problem is solved at an hourly resolution to determine the optimal dispatch of resources that minimizes power shortages while ensuring operational constraints (e.g., transmission capacity and phase angle constraints, quarter-monthly hydro requirements, and battery state transitions) are enforced. Due to the lack of cost-setting generators in the proposed 2040 NYS grid, ACORN does not minimize the cost of operating the system but rather maximizes reliability.

To account for deep uncertainties[50] surrounding natural meteorological variability and technological changes (such as temperature increases, variable energy integration, battery storage expansion, and electrification), we employ the full set of 300 alternative scenarios from Liu et al.[2] These scenarios are generated by sampling a six-dimensional uncertainty space of meteorological and technological parameters using Latin Hypercube Sampling, ensuring uniform coverage of each dimension, and the uncertain parameters and their ranges are summarized in Table 4 of Liu et al.[2] (see also Section 2.3 therein). Using temperature-adjusted meteorological inputs in the model's supply, demand, and transmission modules, the authors construct scenario-specific time series for the availability of intermittent energy resources, electrified demand, and transmission line ampacity. See Liu et al.[2] for further details.

We consider each year of the 22-year simulation period for each alternative meteorological-technological scenario as a different scenario-year, giving us an ensemble of 6,600 scenario-years. Meteorological and technological features for each scenario-year are summarized using anomalies relative to a baseline scenario incorporating changes in generation technology, transmission infrastructure, storage expansion, and load profile detailed in the CLCPA scoping plan[34] but using historical meteorological patterns. For each scenario, we compute the time-averaged anomaly between the scenario-specific time series and the corresponding baseline time series for several statewide quantities: average temperature, solar availability, wind availability, hydro availability, and load. For temperature, solar availability, wind availability, and load, anomalies are computed from hourly time series. Specifically, given a scenario-specific time series $\{x_t\}_{t=1}^{T}$ and the corresponding baseline time series $\{\tilde{x}_t\}_{t=1}^{T}$, we compute the anomaly as the mean of the pointwise difference, $\frac{1}{T}\sum_{t=1}^{T}(x_t - \tilde{x}_t)$, which represents the average hourly deviation from the baseline over the year. Hydro availability anomalies are computed analogously but using quarter-monthly time series, reflecting the temporal resolution at which hydro availability is modeled to account for water management and regulatory constraints.

TE estimation and significance testing

TE[27] is a directed (i.e., asymmetric) measure of predictive information transfer from a source process X to a target process Y. Specifically, TE from X to Y is the mutual information between the previous state variable X^- of source X and the future value Y^+ of target Y, conditioned on the past state variable Y^- of target Y:

$$\begin{aligned} TE(X\to Y) &= I(X^- : Y^+|Y^-) \\ &= \sum_{x^-,y^+,y^-} p(x^-,y^+,y^-)\log\frac{p(y^+|y^-,x^-)}{p(y^+|y^-)}. \end{aligned}$$

This definition assumes X and Y are discrete-valued stationary processes,[25] and there is an analogous definition for continuous-valued processes based on differential entropy.[51]

By conditioning on the past, TE incorporates directional and dynamical information; however, it is a measure only of observed correlation rather than causal effect, which typically requires some perturbation of or intervention in the system to measure.[25] TE is therefore appropriately interpreted as a model-free test statistic for Granger causality, also known as observational causality.[30]

When estimating TE from time-series data, it is convenient if X and Y can be assumed to be stationary processes so that the appropriate probability distributions involving X^-, Y^-, and Y^+ can be estimated from samples over time[25,30] (see Wollstadt et al.[42] and Gómez-Herrero et al.[52] for details on estimating time-dependent TE values from ensembles of time series representing copies of the random processes). Thus, to limit the influence of seasonal trends that could introduce nonstationarity, we restrict our analysis to the summer months—June, July, and August—and scale the time series by relevant capacity as described below.

For each potential predictive pressure point X, we follow a standard procedure[30,53] for estimating pairwise TE from the time series $\{x_t\}_{t=1}^{T}$ measuring utilization of the resource or infrastructure and the time series $\{y_t\}_{t=1}^{T}$ measuring power shortages at the target load bus. We reconstruct the underlying state space for each process by assuming that Y^- and X^- take the form of time-delay embedding vectors[30,42,53] and optimizing the embedding parameters via the Ragwitz criterion[54] (Figure S14). It is standard to take Y^+ to be the value of target Y one time-step in the future. This state space reconstruction step is critical to avoid under- or overestimating $TE(X \rightarrow Y)$. Further details regarding state space reconstruction can be found in the supplemental information.

We estimate $TE(X \rightarrow Y)$ using the Associations.jl Julia package.[55] Time series for resources that predominantly jump between no utilization and full utilization are effectively discrete. In such cases, estimating the relevant probabilities in the TE functional by the frequency of occurrence of different states[30] provides the most consistent results. For continuous-valued processes, state-of-the-art TE estimators use nearest-neighbor estimates of the relevant probability densities with adaptive resolutions to account for the different dimensionalities of the underlying densities.[56] We use the Frenzel-Pompe-Vejmelka-Paluš estimator[57,58] in this case.

Raw TE estimates have limited interpretability because of inherent statistical bias in estimators and because of the varying statistical properties of the underlying time series.[25] Thus, to determine when a TE estimate indicates meaningful information transfer, we rely on a null-hypothesis significance test, estimating the distribution of $TE(X \rightarrow Y)$ under the null hypothesis that there is no predictive information transfer from X to Y and then calculating the p-value for obtaining the sample estimate of $TE(X \rightarrow Y)$ under this null distribution.[25,30] We estimate this null distribution by generating surrogate source time series[59] $\{\hat{x}\}_{t=1}^{T}$ that preserve important statistical properties of the original source time series $\{x\}_{t=1}^{T}$ (Figure S15) and use a significance threshold of 0.05. Further details regarding surrogate generation can be found in the supplemental information. Lowering the significance level reduces the number of predictive pressure points identified in each scenario-year, decreasing the likelihood of false positives but potentially overlooking meaningful interactions. Conversely, increasing the significance level makes the test more permissive, increasing the chance of detecting weaker but possibly spurious correlations.

Simulation data for TE estimation

Hourly time series reflecting curtailment, generation, interface flow, and battery state are used in TE estimates—representing source processes—to identify pressure points at wind and solar generators, hydro generators, transmission interfaces, and batteries, respectively. We consider curtailment as a metric for non-dispatchable energy resource utilization because it is more straightforward to interpret than generation: a lack of generation could reflect either curtailment or unavailability of that resource, while a lack of curtailment indicates that we are fully utilizing that resource's available energy. We consider interface flow across the NYS zonal interfaces to capture transmission utilization instead of individual branch flow because it gives a more comprehensive picture of how power is moving through the grid. Flows through individual branches are noisier and may be highly sensitive to small variations in DC-OPF model parameters.

We scale each time series by the relevant capacity—hourly energy availability and transmission capacity for intermittent energy resources and transmission interfaces, respectively, and installed capacity for hydropower generation and batteries—to reflect when resources are being under- or fully utilized. This captures the weakening of the system due to weather-related stressors. As an example, when extreme temperatures decrease the carrying ampacity of transmission lines, the amount of electricity that can flow through the lines is limited.[36] Any resulting shortage could be associated with the "true" congestion rather than the nominal underutilization. Rescaling to unit range is also important to ensure accurate and stable TE estimates.

The target process in all of our TE estimates is hourly unmet demand (as a proportion of total demand) at a selected zone G bus. This bus was chosen as it consistently experiences the most frequent occurrence and highest proportion of unmet demand across all scenario-years (Figure S4).

Scenario discovery

To identify meteorological and technological features that result in consistent patterns of predictive transmission pressure points, we cluster the results of our TE analysis using the k-modes algorithm, a variation of the k-means algorithm suitable for categorical data.[60,61] For each scenario-year, the flow at each of the 15 transmission interfaces either has or does not have significant TE to the pattern of power shortages at the zone G load bus.

Using a common approach to determine the number of clusters—examining the within-cluster dissimilarity—suggests there could be up to eight distinct clusters (Figures S16 and S17). However, there is considerable overlap across these clusters: for example, four of the largest clusters represent different combinations of predictive pressure points at the A-B, B-C, NYS-PJM, and I-K interfaces. Furthermore, the smaller clusters are considerably less cohesive, suggesting that there is a fraction of scenario-years with atypical combinations of predictive transmission pressure points. Thus, we choose to limit our analysis to three clusters (see Figure 5) representing the most dominant patterns.

We use a classification tree[39] trained using the MLJ.jl Julia package[62] to predict cluster membership using a subset of the meteorological and technological features described above: mean hourly anomaly in temperature, solar availability, wind availability, and hydro availability as well as battery capacity scaling factor. We exclude the mean hourly load anomaly, as this is almost perfectly correlated with the mean hourly anomaly in temperature (Figure S3B). To avoid potential overfitting, we limit the depth of the tree to three levels. The fitted classification tree is in Figure S18. As discussed in the results, this tree is a relatively weak classifier. The balanced accuracy[63] is 51.4%, which represents a fairly small improvement over random guessing. A classification tree for predicting membership among the full eight clusters is also a weak classifier. The balanced accuracy for a tree with four levels is 30.7%—again, a small improvement over random guessing.

RESOURCE AVAILABILITY

Lead contact

Requests for further information and resources should be directed to and will be fulfilled by the lead contact, Katerina Tang (kbt28@cornell.edu).

Materials availability

This study did not generate any new, unique materials.

Data and code availability

The code used in this study, along with data for the three base scenarios, is archived at https://doi.org/10.5281/zenodo.16783066. Data used in the scenario discovery subsection are based on simulations produced using the publicly available ACORN model (https://github.com/AndersonEnergyLab-Cornell/ny-clcpa2050), and the analysis scripts required to reproduce our scenario discovery results are included in the Zenodo archive.

ACKNOWLEDGMENTS

K.T. and V.S. were partially supported for this research by the US Department of Energy, Office of Science, Biological and Environmental Research Program, Earth and Environmental Systems Modeling, and MultiSector Dynamics under Cooperative Agreement DE-SC0022141. This research was also conducted with support from the Cornell University Center for Advanced Computing, which receives funding from Cornell University, the National Science Foundation, and members of its Partner Program. The authors would like to thank David Lafferty, Parin Bhaduri, and other members of the Srikrishnan Lab Group for their help and insights.

AUTHOR CONTRIBUTIONS

K.T., conceptualization, methodology, formal analysis, visualization, and writing – original draft. M.V.L., data curation and writing – reviewing & editing. C.L.A., supervision and writing – reviewing & editing. V.S., conceptualization, supervision, and writing – reviewing & editing.

DECLARATION OF INTERESTS

The authors declare no competing interests.

SUPPLEMENTAL INFORMATION

Supplemental information can be found online at https://doi.org/10.1016/j.crsus.2026.100660.

Received: August 15, 2025
Revised: January 7, 2026
Accepted: February 16, 2026
Published: March 26, 2026

REFERENCES

1. Craig, M.T., Wohland, J., Stoop, L.P., Kies, A., Pickering, B., Bloomfield, H.C., Browell, J., De Felice, M., Dent, C.J., Deroubaix, A., et al. (2022). Overcoming the disconnect between energy system and climate modeling. Joule *6*, 1405–1417. https://doi.org/10.1016/j.joule.2022.05.010.
2. Liu, M.V., Srikrishnan, V., Doering, K., Kabir, E., Steinschneider, S., and Anderson, C.L. (2025). Energy system vulnerabilities in a zero-emission grid: The role of climate variability and technology uncertainty. Energy *335*, 137937. https://doi.org/10.1016/j.energy.2025.137937.
3. Grochowicz, A., Van Greevenbroek, K., and Bloomfield, H.C. (2024). Using power system modelling outputs to identify weather-induced extreme events in highly renewable systems. Environ. Res. Lett. *19*, 054038. https://doi.org/10.1088/1748-9326/ad374a.
4. Xu, L., Feng, K., Lin, N., Perera, A.T.D., Poor, H.V., Xie, L., Ji, C., Sun, X.A., Guo, Q., and O'Malley, M. (2024). Resilience of renewable power systems under climate risks. Nat. Rev. Electr. Eng. *1*, 53–66. https://doi.org/10.1038/s44287-023-00003-8.
5. Otero, N., Martius, O., Allen, S., Bloomfield, H., and Schaefli, B. (2022). Characterizing renewable energy compound events across Europe using a logistic regression-based approach. Meteorol. Appl. *29*, e2089. https://doi.org/10.1002/met.2089. https://onlinelibrary.wiley.com/doi/pdf/10.1002/met.2089.
6. Webster, M., Fisher-Vanden, K., Kumar, V., Lammers, R.B., and Perla, J. (2022). Integrated hydrological, power system and economic modelling of climate impacts on electricity demand and cost. Nat. Energy *7*, 163–169. https://doi.org/10.1038/s41560-021-00958-8.
7. Bernstein, A., Bienstock, D., Hay, D., Uzunoglu, M., and Zussman, G. (2014). Power grid vulnerability to geographically correlated failures—analysis and control implications. In IEEE Conference on Computer Communications, pp. 2634–2642. https://doi.org/10.1109/INFOCOM.2014.6848211.
8. Shuvro, R.A., Das, P., Wang, Z., Rahnamay-Naeini, M., and Hayat, M.M. (2018). Impact of initial stressor(s) on cascading failures in power grids. In 2018 North American Power Symposium (NAPS), pp. 1–6. https://doi.org/10.1109/NAPS.2018.8600585.
9. Hines, P.D.H., Dobson, I., and Rezaei, P. (2016). Cascading Power Outages Propagate Locally in an Influence Graph That is Not the Actual Grid Topology. IEEE Trans. Power Syst. *32*, 958–967. https://doi.org/10.1109/TPWRS.2016.2578259.
10. Yang, Y., Nishikawa, T., and Motter, A.E. (2017). Small vulnerable sets determine large network cascades in power grids. Science *358*, eaan3184. https://doi.org/10.1126/science.aan3184.
11. Ghasemi, A., and Kantz, H. (2022). Higher-order interaction learning of line failure cascading in power networks. Chaos *32*, 073101. https://doi.org/10.1063/5.0089780.
12. Bompard, E., Napoli, R., and Xue, F. (2009). Analysis of structural vulnerabilities in power transmission grids. Int. J. Crit. Infrastruct. Prot. *2*, 5–12. https://doi.org/10.1016/j.ijcip.2009.02.002.
13. Wang, Z., Scaglione, A., and Thomas, R.J. (2010). Electrical centrality measures for electric power grid vulnerability analysis. In 49th IEEE Conference on Decision and Control (CDC), pp. 5792–5797, ISSN 0191-2216. https://doi.org/10.1109/CDC.2010.5717964.
14. Zio, E., and Golea, L.R. (2012). Analyzing the topological, electrical and reliability characteristics of a power transmission system for identifying its critical elements. Reliab. Eng. Syst. Saf. *101*, 67–74. https://doi.org/10.1016/j.ress.2011.11.009.
15. Liu, B., Li, Z., Chen, X., Huang, Y., and Liu, X. (2018). Recognition and Vulnerability Analysis of Key Nodes in Power Grid Based on Complex Network Centrality. IEEE Trans. Circuits Syst. II Express Briefs *65*, 346–350. https://doi.org/10.1109/TCSII.2017.2705482.
16. Fan, B., Shu, N., Li, Z., and Li, F. (2023). Critical Nodes Identification for Power Grid Based on Electrical Topology and Power Flow Distribution. IEEE Syst. J. *17*, 4874–4884. https://doi.org/10.1109/JSYST.2022.3227632.
17. Beyza, J., Garcia-Paricio, E., Ruiz, H.F., and Yusta, J.M. (2021). Geodesic Vulnerability Approach for Identification of Critical Buses in Power Systems. J. Mod. Power Syst. Clean Energy *9*, 37–45. https://doi.org/10.35833/MPCE.2018.000779.
18. Rodríguez, R.A., Becker, S., Andresen, G.B., Heide, D., and Greiner, M. (2014). Transmission needs across a fully renewable european power system. Renew. Energy *63*, 467–476. https://doi.org/10.1016/j.renene.2013.10.005.
19. Schlachtberger, D.P., Brown, T., Schramm, S., and Greiner, M. (2017). The benefits of cooperation in a highly renewable european electricity network. Energy *134*, 469–481. https://doi.org/10.1016/j.energy.2017.06.004.
20. Chen, X., Lv, J., McElroy, M.B., Han, X., Nielsen, C.P., and Wen, J. (2018). Power system capacity expansion under higher penetration of renewables considering flexibility constraints and low carbon policies. IEEE Trans. Power Syst. *33*, 6240–6253. https://doi.org/10.1109/TPWRS.2018.2827003.
21. Sepulveda, N.A., Jenkins, J.D., De Sisternes, F.J., and Lester, R.K. (2018). The role of firm low-carbon electricity resources in deep decarbonization of power generation. Joule *2*, 2403–2420. https://doi.org/10.1016/j.joule.2018.08.006.

22. Jirutitijaroen, P., and Singh, C. (2008). Reliability constrained multi-area adequacy planning using stochastic programming with sample-average approximations. In 2008 IEEE Power and Energy Society General Meeting – Conversion and Delivery of Electrical Energy in the 21st Century, p. 1. https://doi.org/10.1109/PES.2008.4596575.

23. Aghaei, J., Amjady, N., Baharvandi, A., and Akbari, M.A. (2014). Generation and transmission expansion planning: MILP–based probabilistic model. IEEE Trans. Power Syst. *29*, 1592–1601. https://doi.org/10.1109/TPWRS.2013.2296352.

24. Dehghan, S., Amjady, N., and Conejo, A.J. (2016). Reliability-constrained robust power system expansion planning. IEEE Trans. Power Syst. *31*, 2383–2392. https://doi.org/10.1109/TPWRS.2015.2464274.

25. Bossomaier, T., Barnett, L., Harré, M., and Lizier, J.T. (2016). An Introduction to Transfer Entropy (Springer International Publishing), ISBN 978-3-319-43221-2. https://doi.org/10.1007/978-3-319-43222-9.

26. Vicente, R., Wibral, M., Lindner, M., and Pipa, G. (2011). Transfer entropy—a model-free measure of effective connectivity for the neurosciences. J. Comput. Neurosci. *30*, 45–67. https://doi.org/10.1007/s10827-010-0262-3.

27. Schreiber, T. (2000). Measuring Information Transfer. Phys. Rev. Lett. *85*, 461–464. https://doi.org/10.1103/PhysRevLett.85.461.

28. Yang, Y., Nishikawa, T., and Motter, A.E. (2017). Vulnerability and Cosusceptibility Determine the Size of Network Cascades. Phys. Rev. Lett. *118*, 048301. https://doi.org/10.1103/PhysRevLett.118.048301.

29. Qi, J., Wang, J., and Sun, K. (2018). Efficient estimation of component interactions for cascading failure analysis by EM algorithm. IEEE Trans. Power Syst. *33*, 3153–3161. https://doi.org/10.1109/TPWRS.2017.2764041.

30. Wibral, M., Vicente, R., and Lindner, M. (2014). Transfer Entropy in Neuroscience. In Directed Information Measures in Neuroscience. Understanding Complex Systems, M. Wibral, R. Vicente, and J.T. Lizier, eds. (Springer Berlin Heidelberg), pp. 3–36, ISBN 978-3-642-54473-6 978-3-642-54474-3, 3–36. https://doi.org/10.1007/978-3-642-54474-3_1.

31. Runge, J., Heitzig, J., Petoukhov, V., and Kurths, J. (2012). Escaping the Curse of Dimensionality in Estimating Multivariate Transfer Entropy. Phys. Rev. Lett. *108*, 258701. https://doi.org/10.1103/PhysRevLett.108.258701.

32. McManamay, R.A., Brinkley, C., Vernon, C.R., Raj, S., and Rice, J.S. (2022). Urban land teleconnections in the united states: A graphical network approach. Comput. Environ. Urban Syst. *95*, 101822. https://doi.org/10.1016/j.compenvurbsys.2022.101822.

33. Dimpfl, T., and Peter, F.J. (2013). Using transfer entropy to measure information flows between financial markets. Stud. Nonlinear Dyn. Econ. *17*, 85–102. https://doi.org/10.1515/snde-2012-0044.

34. New York State Climate Action Council. (2022). New York State Climate Action Council Scoping Plan. Tech. Rep. climate.ny.gov/ScopingPlan.

35. Kabir, E., Srikrishnan, V., Liu, M.V., Steinschneider, S., and Anderson, C.L. (2024). Quantifying the impact of multi-scale climate variability on electricity prices in a renewable-dominated power grid. Renew. Energy *223*, 120013. https://doi.org/10.1016/j.renene.2024.120013.

36. Bartos, M., Chester, M., Johnson, N., Gorman, B., Eisenberg, D., Linkov, I., and Bates, M. (2016). Impacts of rising air temperatures on electric transmission ampacity and peak electricity load in the United States. Environ. Res. Lett. *11*, 114008. https://doi.org/10.1088/1748-9326/11/11/114008.

37. Levin, T., Bistline, J., Sioshansi, R., Cole, W.J., Kwon, J., Burger, S.P., Crabtree, G.W., Jenkins, J.D., O'Neil, R., Korpås, M., et al. (2023). Energy storage solutions to decarbonize electricity through enhanced capacity expansion modelling. Nat. Energy *8*, 1199–1208. https://doi.org/10.1038/s41560-023-01340-6.

38. Kwakkel, J.H., Haasnoot, M., and Walker, W.E. (2015). Developing dynamic adaptive policy pathways: a computer-assisted approach for developing adaptive strategies for a deeply uncertain world. Clim. Change *132*, 373–386. https://doi.org/10.1007/s10584-014-1210-4.

39. Breiman, L., Friedman, J.H., Olshen, R.A., and Stone, C.J. (2017). Classification and Regression Trees (Chapman and Hall/CRC). https://doi.org/10.1201/9781315139470.

40. DeCarolis, J.F. (2011). Using modeling to generate alternatives (mga) to expand our thinking on energy futures. Energy Econ. *33*, 145–152. https://doi.org/10.1016/j.eneco.2010.05.002.

41. Lombardi, F., Van Greevenbroek, K., Grochowicz, A., Lau, M., Neumann, F., Patankar, N., and Vågerö, O. (2025). Near-optimal energy planning strategies with modeling to generate alternatives to flexibly explore practically desirable options. Joule *9*, 102144. https://doi.org/10.1016/j.joule.2025.102144.

42. Wollstadt, P., Martínez-Zarzuela, M., Vicente, R., Díaz-Pernas, F.J., and Wibral, M. (2014). Efficient Transfer Entropy Analysis of Non-Stationary Neural Time Series. PLoS One *9*, e102833. https://doi.org/10.1371/journal.pone.0102833.

43. Lizier, J.T., and Rubinov, M. (2012). Multivariate construction of effective computational networks from observational data. Preprint at MiS Preprints https://www.mis.mpg.de/publications/preprint-repository/article/2012/issue-25.

44. Faes, L., Nollo, G., and Porta, A. (2011). Information-based detection of nonlinear Granger causality in multivariate processes via a nonuniform embedding technique. Phys. Rev. E Stat. Nonlin. Soft Matter Phys. *83*, 051112. https://doi.org/10.1103/PhysRevE.83.051112.

45. Novelli, L., Wollstadt, P., Mediano, P., Wibral, M., and Lizier, J.T. (2019). Large-scale directed network inference with multivariate transfer entropy and hierarchical statistical testing. Netw. Neurosci. *3*, 827–847. https://doi.org/10.1162/netn_a_00092.

46. Becker, M., Nassar, H., Espinosa, C., Stelzer, I.A., Feyaerts, D., Berson, E., Bidoki, N.H., Chang, A.L., Saarunya, G., Culos, A., et al. (2023). Large-scale correlation network construction for unraveling the coordination of complex biological systems. Nat. Comput. Sci. *3*, 346–359. https://doi.org/10.1038/s43588-023-00429-y.

47. Casadiego, J., Nitzan, M., Hallerberg, S., and Timme, M. (2017). Model-free inference of direct network interactions from nonlinear collective dynamics. Nat. Commun. *8*, 2192. https://doi.org/10.1038/s41467-017-02288-4.

48. Runge, J., Nowack, P., Kretschmer, M., Flaxman, S., and Sejdinovic, D. (2019). Detecting and quantifying causal associations in large nonlinear time series datasets. Sci. Adv. *5*, eaau4996. https://doi.org/10.1126/sciadv.aau4996.

49. Liu, M.V., Yuan, B., Wang, Z., Sward, J.A., Zhang, K.M., and Anderson, C.L. (2022). An Open Source Representation for the NYS Electric Grid to Support Power Grid and Market Transition Studies. IEEE Trans. Power Syst., 1–11. https://doi.org/10.1109/TPWRS.2022.3200887.

50. Srikrishnan, V., Lafferty, D.C., Wong, T.E., Lamontagne, J.R., Quinn, J.D., Sharma, S., Molla, N.J., Herman, J.D., Sriver, R.L., Morris, J.F., et al. (2022). Uncertainty Analysis in Multi-Sector Systems: Considerations for Risk Analysis, Projection, and Planning for Complex Systems. Earths Future *10*, e2021EF002644. https://doi.org/10.1029/2021EF002644.

51. Kaiser, A., and Schreiber, T. (2002). Information transfer in continuous processes. Phys. D, Nonlinear Phenom. *166*, 43–62. https://doi.org/10.1016/S0167-2789(02)00432-3.

52. Gómez-Herrero, G., Wu, W., Rutanen, K., Soriano, M., Pipa, G., and Vicente, R. (2015). Assessing Coupling Dynamics from an Ensemble of Time Series. Entropy *17*, 1958–1970. https://doi.org/10.3390/e17041958.

53. Lindner, M., Vicente, R., Priesemann, V., and Wibral, M. (2011). TRENTOOL: A Matlab open source toolbox to analyse information flow in time series data with transfer entropy. BMC Neurosci. *12*, 119. https://doi.org/10.1186/1471-2202-12-119.

54. Ragwitz, M., and Kantz, H. (2002). Markov models from data by simple nonlinear time series predictors in delay embedding spaces. Phys. Rev. E Stat. Nonlin. Soft Matter Phys. *65*, 056201. https://doi.org/10.1103/PhysRevE.65.056201.

55. Haaga, K.A. (2025). Associations.jl [source code]. Zenodo. https://doi.org/10.5281/zenodo.7689018.
56. Kraskov, A., Stögbauer, H., and Grassberger, P. (2004). Estimating mutual information. Phys. Rev. E Stat. Nonlin. Soft Matter Phys. *69*, 066138. https://doi.org/10.1103/PhysRevE.69.066138.
57. Frenzel, S., and Pompe, B. (2007). Partial Mutual Information for Coupling Analysis of Multivariate Time Series. Phys. Rev. Lett. *99*, 204101. https://doi.org/10.1103/PhysRevLett.99.204101.
58. Vejmelka, M., and Paluš, M. (2008). Inferring the directionality of coupling with conditional mutual information. Phys. Rev. E Stat. Nonlin. Soft Matter Phys. *77*, 026214. https://doi.org/10.1103/PhysRevE.77.026214.
59. Keylock, C.J. (2006). Constrained surrogate time series with preservation of the mean and variance structure. Phys. Rev. E Stat. Nonlin. Soft Matter Phys. *73*, 036707. https://doi.org/10.1103/PhysRevE.73.036707.
60. Ng, M.K., Li, M.J., Huang, J.Z., and He, Z. (2007). On the Impact of Dissimilarity Measure in k-Modes Clustering Algorithm. IEEE Trans. Pattern Anal. Mach. Intell. *29*, 503–507. https://doi.org/10.1109/TPAMI.2007.53.
61. Huang, Z. (1998). Extensions to the k-Means Algorithm for Clustering Large Data Sets with Categorical Values. Data Min. Knowl. Discov. *2*, 283–304. https://doi.org/10.1023/A:1009769707641.
62. Blaom, A.D., Kiraly, F., Lienart, T., Simillides, Y., Arenas, D., and Vollmer, S.J. (2020). MLJ: A julia package for composable machine learning. J. Open Source Softw. *5*, 2704. https://doi.org/10.21105/joss.02704.
63. Mosley, L. (2013). A Balanced Approach to the Multi-class Imbalance Problem. PhD thesis (Iowa State University).